CHAPTER 4

Misdirection of regenerating motor axons after nerve injury and repair in the rat sciatic nerve model

Godard C.W. de Ruiter [1,2,3], Martijn J.A. Malessy [3], Awad O Alaid [1], Robert J. Spinner [2], JaNean K Engelstad [4], Eric J. Sorenson [5], Kenton R. Kaufman [6], Peter J. Dyck [4], Anthony J. Windebank [1]

[1] Laboratory for Molecular Neuroscience, Mayo Clinic, Rochester MN, USA
[2] Department of Neurologic Surgery, Mayo Clinic Rochester MN, USA
[3] Department of Neurosurgery, Leiden University Medical Center, the Netherlands
[4] Laboratory for Peripheral Nerve Research, Mayo Clinic, Rochester MN, USA
[5] Department of Clinical Neurophysiology, Mayo Clinic, Rochester MN, USA
[6] Laboratory for Motion analysis, Mayo Clinic, Rochester MN, USA

Published in Experimental Neurology
2008, Volume 211(2); 339-350

ABSTRACT

Background Misdirection of regenerating axons is one of the factors that can explain the poor results often found after nerve injury and repair. Little is known however about the exact impact of misdirection. In this study, we quantified the degree of misdirection and the effect on recovery of function after different types of nerve injury and repair in the rat sciatic nerve model; crush injury, direct coaptation, and autologous nerve graft repair.

Methods Sequential tracing with retrograde labeling of the peroneal nerve before and 8 weeks after nerve injury and repair was performed to quantify the accuracy of motor axon regeneration. Digital video analysis of ankle motion was used to investigate the recovery of function. In addition, serial compound action potential recordings and nerve and muscle morphometry were performed.

Results In our study, accuracy of motor axon regeneration was found to be limited; only 71% (±4.9%) of the peroneal motoneurons were correctly directed 2 months after sciatic crush injury, 42% (±4.2%) after direct suture, and 25% (±6.6%) after autograft repair. Recovery of ankle motion was incomplete after all types of nerve injury and repair and demonstrated a disturbed balance of ankle plantar and dorsiflexion. The number of motoneurons from which axons had regenerated was not significantly different from normal. The number of myelinated axons was significantly increased distal to the site of injury.

Conclusion Misdirection of regenerating motor axons is a major factor in the poor recovery of nerves that innervate different muscles. The results of this study can be used as basis for developing new nerve repair techniques that may improve accuracy of regeneration.

INTRODUCTION

Functional results after nerve injury and repair are often disappointing [1]. Several factors that influence the results of regeneration have been identified, including the type of injury (sharp or blunt trauma or traction), location of the injury, time between the injury and surgery [2, 3], and the age of the patient. Misdirection of regenerating axons is also a factor that may explain poor functional recovery [4]. After repair of motor nerves, misdirection may lead to cocontraction of muscles or synkinesis. After repair of a sensory nerve, misdirection may lead to disturbed sensory function even years after the injury [5].

Misdirection has been investigated experimentally with different tools and techniques, including Y-shaped tubes [6, 7], selective muscle contraction measurements [8, 9], and compound muscle action potentials [10]. Different retrograde tracing techniques have also been used to investigate the accuracy of motor and sensory regeneration, including single labeling [11-13], simultaneous double labeling [14-16] and sequential double labeling [17, 18], and recently, a new technique that uses mice

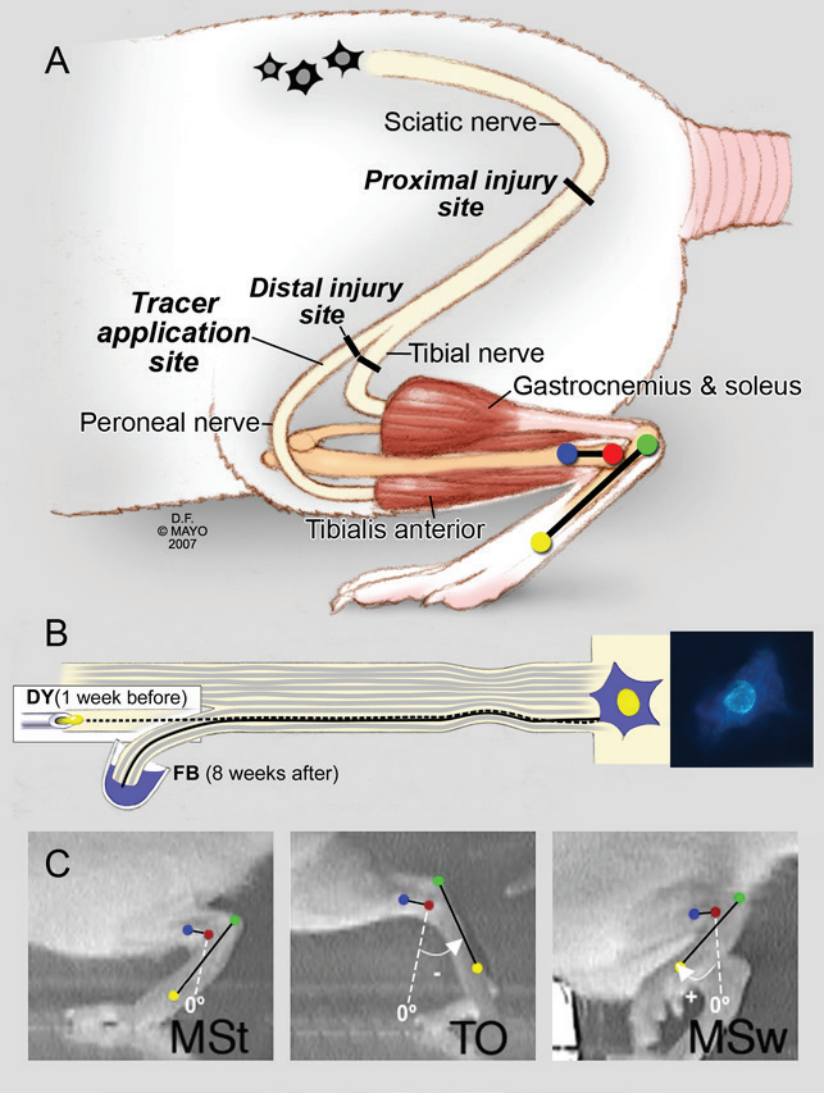

Figure 1

A, The rat sciatic nerve model with distal tibial and peroneal nerve branches that respectively innervate the gastrocnemic-soleus and anterior tibial muscles for ankle plantar and dorsiflexion. The proximal site of injury for all types of nerve injury and repair, the distal site of injury for autograft repair, and the site of tracer application are shown. B, Sequential retrograde tracing technique with injection of the first tracer (diamidino yellow [DY] into the peroneal nerve 1 week before nerve injury and the second tracer (fast blue [FB]) 8 weeks after nerve injury and repair. C, 2D digital video analysis of the ankle angles at midstance (MSt), toe-off (TO), and midswing (MSw), reported in degrees from neutral position, with plantar flexion being negative and dorsiflexion being positive.

with a fluorescent marker in a subset of their axons, has been introduced [19, 20]. The results of these studies all suggest that accuracy of regeneration is limited. However, little is known about the extent of misdirection and the effect on the recovery of function, especially in the repair of motor nerves innervating different distal target muscles. This becomes of more interest as new repair techniques that may more accurately guide regeneration become available (e.g. selective nerve growth factors and nerve guides with a more complex microarchitecture).

In this study we investigated misdirection in the rat sciatic nerve model after different types of nerve injury; crush injury vs transection injury, and repair techniques; direct coaptation vs autograft repair (in clinical practice, direct coaptation repair is always attempted first in case of a transection injury; in case a nerve graft is needed to bridge a defect, the autograft is still the gold standard of repair). Two recently introduced methods were used to evaluate results: sequential retrograde tracing [21-24] and digital video ankle motion analysis [25] (**Chapter 3**). Sequential retrograde tracing was performed to quantify the accuracy of motor axons for regeneration to the original target nerve (Figure 1). Ankle motion was analyzed to investigate the effect of misdirection on the recovery of function. Markers placed on the leg of the rat were automatically tracked for the change in ankle angle (Figure 1). Ankle motion analysis is sensitive in detecting differences in effect on ankle plantar flexion and dorsiflexion after separate sciatic, tibial, and peroneal nerve crush injuries [25]. Also, it is a more sensitive method than the sciatic function index, currently the standard method for assessment of function in the rat sciatic nerve model. In addition, compound muscle action potential (CMAP) recordings were made every other week, nerve and muscle morphometry were performed at the end of the experiment, and correlations between results of the different evaluation methods were investigated.

The results presented in this study can be used as a baseline for future experiments that focus on the improvement of regeneration after nerve injury and repair.

MATERIAL AND METHODS

Experimental groups

All animals (*n*=34), Sprague-Dawley rats (250-275 g), were randomly assigned to one of the experimental groups of crush injury, direct coaptation, or autograft repair. In the sequential tracing experiment, 4 animals per group were used. In 4 animals, the efficacy of the tracing method was determined on the contralateral side. In the motion analysis experiment, 5 animals per group were used and normal ankle motion was analyzed in 3 control animals. CAMP recordings and nerve and muscle morphometry were performed in the animals used in the motion analysis experiment (except for the control values that were obtained from a different experiment, **Chapter 7** [26]). All procedures were approved by the Institutional Ani-

mal Care and Use Committee and performed according to the animal care guidelines of the Mayo Foundation.

Surgical procedures and post-operative care

Animals were anesthetized by intraperitoneal injection of a mixture of 80 mg/kg ketamine and 2.5mg/kg xylazine. The sciatic nerve was exposed through a dorsal gluteal-splitting approach with the aid of a Zeiss operating microscope. The nerve was either crushed by applying maximal force with a smooth forceps for 5 seconds or transected with sharp microscissors 2mm distally from the white line formed by the fascia of the paraspinal muscles. The transection injury was repaired immediately with 4 10-0 monofilament sutures (Ethicon, Inc, Somerville, New Jersey). For the autograft repair, in addition to the proximal transection injury site, a second transection injury site was made 1 cm distally by transection of the tibial and peroneal branches (Figure 1A). Both injury sites were repaired microsurgically. For the distal repair site, the tibial and peroneal nerves were repaired separately with 4 and 2 10-0 sutures, respectively. The wound was closed in layers. Buprenorphine hydrochloride (Reckitt Benckiser Healthcare, Slough, United Kingdom) was administered subcutaneously just before and 12 hours after the repair for prevention of pain. During follow-up period, animals were housed separately in cages, with a 12-hour light-dark cycle. Water and food were available *ad libitum*. The hindlimbs that were operated on were sprayed daily with Chewguard (Butler Corporation, Greensboro, North Carolina) to prevent autotomy. A wire mesh was placed inside the cages for cage exercise enrichment and to prevent contractures [27]. In addition, manual physiotherapy (by passively moving the ankle) was performed once a week.

Sequential retrograde tracing

One week before injury, 1µl of 5% diamidino yellow (DY) solution (EMS-Chemie, GRoß-Umstadt, Germany) was injected, with a 25-gauge needle attached to a scaled Hamilton syringe, into the peroneal nerve (15 mm from the intended injury site) (Figure 1B). Eight weeks after injury, the peroneal nerve was transected proximal to the injection site of DY tracer, and the proximal end was placed in 1.5µl of 5% fast blue (FB) solution (EMS-Chemie) for 30 min. After the application of FB, the nerve stump was cleaned with 0.9% saline and sutured into surrounding fat tissue to prevent leakage of the tracer. (The method of preventing tracer leakage was validated in normal animals, after which no double-labeled profiles were found). The same procedures and time intervals were used to determine the labeling efficiency in control animals. Six days after application of FB tracer, the animals were perfused with phosphate-buffered saline (PBS) and 4% paraformaldehyde in 10% sucrose solution. Spinal cord segments L1-6 were removed and post-fixed overnight in a solution of 15% sucrose in PBS. Tissue was embedded in Tissue Freezing medium (TFM; TBS, Durham, North Carolina) and stored at -80ºC until sectioning.

Longitudinal 30-μm-thick sections were cut on a cryostat at -20 ºC. Slides were evaluated immediately with a fluorescent microscope (Axioplan 2, Carl Zeiss, Inc. Oberkochen, Germany) with a DAPI filter set (360/400-nm band-pass excitation filter, 440 nm long-pass emission filter, and 400-nm dichroic beam splitter) at x20 magnification with a Plan Apochromat 20x/0.75 objective (Carl Zeiss, Inc). Neuronal profiles were counted in every section by an observer blinded to the experimental groups. Only profiles with a visible nucleus were counted. Profiles with blue cytoplasm and dark nuclei were counted as FB-labeled cells, and those with yellow nuclei and dark cytoplasm as DY-labeled cells. Profiles with blue cytoplasm and yellow nuclei were counted as double-labeled FB-DY cells (Figure 1). No corrections were made for lost caps of motoneuron nuclei or double counting of split motoneuron nuclei. The total number of regenerated profiles was calculated by adding the number of single FB-labeled and double FB-DY-labeled profiles. The percentage correctly directed peroneal motoneurons was calculated by dividing the number of double-labeled profiles by the total number of DY-labeled profiles (single- and double-labeled DY). Labeling efficiency was determined from the percentage double labeling in normal animals. Spinal distributions of profiles (rostrocaudal and anteroposterior) were microscopically analyzed in all sections.

2D digital video ankle motion analysis

Ankle motion was analyzed 1 week after nerve injury and repair every other week starting 2 weeks after sciatic nerve crush injury and 4 weeks after direct coaptation and autograft repair. For the analysis of ankle motion, rats were briefly anesthetized with isoflurane inhalation (Abbott Animal Health, North Chicago, Illinois). The left leg was shaved. Black dot markers (Sharpie, Sanford Manufacturing, Chicago, Illinois) were placed on bony landmarks of the tibia, lateral malleolus, calcaneus, and fifth metatarsal to create a 2D biomechanical model of the ankle (Figure 1). For detailed description of ankle motion analysis see **Chapter 3**.

In short: Animals were placed in a transparent runway (120cm long, 12cm wide, 30cm high) and filmed using a 60-Hz digital camera (Dinion ^{XF} CCD Camera; Bosch Security Systems) that was positioned on a tripod 1 m perpendicular to the runway. Rats were trained to walk inside the runway by shifting a black box from one end to the other. Trials of the rat running from the right to the left side were selected because of the presence of 1 complete step cycle and a total duration of the step cycle of 0.25 to 0.50 s. After filming, the digital videos were processed using motion analysis software (Vicon Peak, Centennial, Colorado) that automatically tracks the markers on the leg of the rat in each frame of the video. The data were filtered with a Butterworth filter set at 6 Hz recorded with Vicon software. The results of ankle motion after crush injury, direct coaptation, and autograft repair were compared for the value of the ankle angle at different moments during the step cycle: midstance (MSt), the moment the right foot in the air crosses the left foot in the stance (that bears the weight); toe off (TO), the moment the left foot comes off the runway (in normal animals, the moment of maximum plantar

flexion); and midswing (MSw), the moment the left foot crosses the right foot in the stance (in normal animals, the moment of maximum dorsiflexion). Data for the ankle angles were reported in degrees from the neutral position of the ankle angel (the plantar surface of the foot perpendicular to the tibia, with dorsiflexion being positive and plantar flexion being negative (Figure 1C).

Compound muscle action potential recording

After the animals were filmed, they were (again) briefly anesthetized with ketamine and xylazine. CMAPs were recorded in the tibial- and peroneal nerve-innervated foot muscles using a Nicolet Viking IV EMG machine (Viasys NeuroCare, Madison, Wisconsin). Fine needle electrodes were placed in the injured/operated leg of the rat; recording electrodes were placed directly posterior to the tibia, with approximately 5 mm between the distal cathode and proximal anode. The simulating electrodes were adjusted locally to produce maximal CMAP amplitude. The stimulus was increased incrementally to produce a supramaximal response.

Nerve morphometry

At the end of the follow-up period (16 weeks), the sciatic nerve was reexposed and fixed in situ with 2.5% glutaraldehyde in PBS for 30 min [28]. A 1-mm nerve segment was transected/selected 2 mm distal to the site of injury. The nerve specimen was immersed (immediately) in glutaraldehyde overnight and postfixed in 1% osmium tetroxide and embedded in spur resin. Semithin (1 μm) sections were cut on a ultramicrotome with a glass knife and stained with 1% *p*-phenylenediamine. Sections were analyzed with the imaging system for nerve morphometry [28] for the total number of myelinated fibers/nerve, mean size and size distribution of myelinated fibers, and mean myelin thickness [28].

Muscle morphometry

For analysis of the total muscle fiber surface area and mean muscle fiber size after nerve injury and repair, the soleus muscle was resected from the left limb and imbedded in tissue freezing medium (TBS) using isopentane and liquid nitrogen. Transverse 10-μm-thick sections were cut on a cryostat (at -20 °C) from the midbelly of the muscle and were stained for myofibrillar ATPase (at pH 9.4) according to the method described by Brooke and Kaiser [29], which stains slow (type I) fibers light and fast (type II) fibers dark. The total muscle fiber surface area (without areas of fibrosis or vessels) was determined with the KS400 system (Zeiss, Version 3.0) [30]. The number of type I and type II fibers was counted in every section. The mean muscle fiber size was calculated from the muscle fiber surface area and the total number of muscle fibers.

Statistical Analysis

All results are reported as the mean ± SD, unless stated otherwise. The 2-tailed Student *t* test was used for comparisons between 2 groups, with the assumption

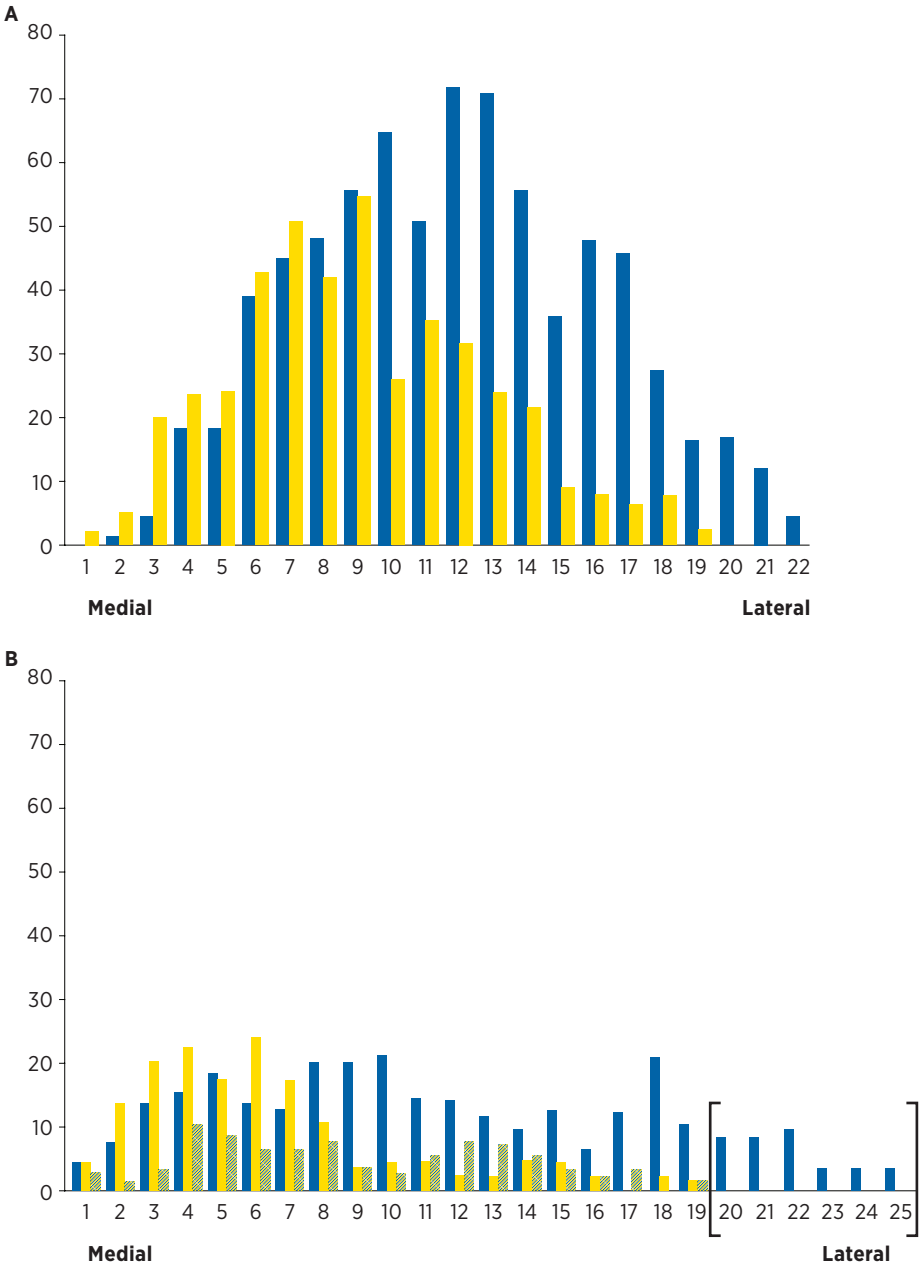

Figure 2

Distribution of differently labeled profiles (diamidino yellow [DY], fast blue [FB], and FB-DY) for the number of profiles per longitudinal section taken from medial to lateral through the anterior horn. A, Normal distribution of tibial (blue) and peroneal (yellow) motoneurons after simultaneous tracing, with FB and DY application tot the tibial and peroneal nerve branches, respectively. B, Distribution of profiles labeled by sequential tracing 8 weeks after autograft repair. In this case there were no signs of reuptake of persistent DY tracer because no double-labeled profiles were found in the area of the anterior horn normally exclusively occupied by tibial motoneurons (indicated by brackets, compare to A).

Table 1

Comparison of single-labeled FB and DY and double-Labeled FB-DY profiles in normal animals, and after crush injury, direct coaptation, and autograft repair

	profiles, mean no. ± SD				labeling efficacy, mean % (±SD)	percentage of correctly directed profiles,† mean % (±SD)
group*	FB	DY	FB-DY	Total		
normal	12 ± 13	25 ± 10	389 ± 49	427 ± 54	91.3 (±2.4)	..
crush injury	95 ± 115	120 ± 79	281 ± 36	376 ± 69	..	71.4 (±4.9)
direct coaptation repair	92 ± 54	338 ± 48	250 ± 73	342 ± 92	..	42.0 (±4.2)
autograft repair	99 ± 14	230 ± 74	73 ± 8	372 ± 17	..	25.1 (±6.6)

DY, diamidino yellow; FB, fast blue.

*each group included 4 animals.

†The percentage of correctly directed profiles was calculated for the total number of double-labeled (FB-DY) profiles divided by the total number of DY-labeled profiles: FB–DY/(FB–DY + DY).

that the data were normally distributed. Repeated measures ANOVA was used for comparison of 3 or more groups.

Linear correlations (Pearson) were investigated between the mean percentages of correctly directed peroneal motoneurons and the mean ankle angles at 8 and 16 weeks after crush injury, direct coaptation, and autograft repair. Linear correlations were also investigated between the mean quantitative results of regeneration and the mean ankle angle at 16 weeks.

RESULTS

Sequential retrograde tracing

The distribution of retrogradely labeled profiles within the anterior horn of the spinal cord after sequential tracing of the peroneal nerve was changed after nerve injury and repair compared with the normal distribution of peroneal motoneurons in control animals; single-labeled FB profiles were also present or found in an area that normally is occupied exclusively by tibial motoneurons, suggesting misdirection of regenerating axons originating from the tibial motoneuron pool into the peroneal nerve branch (Figure 2). This area was also used to exclude extreme cases of DY tracer reuptake; the presence of double-labeled FB-DY profiles in this area would indicate re-uptake of persistent DY tracer by misdirected axons from the tibial motoneurons. In no case were double labeled FB-DY profiles found in this area.

The number of FB, DY, and FB-DY profiles counted after crush injury, direct coaptation repair, and autograft repair is listed in Table 1. The number of single-labeled

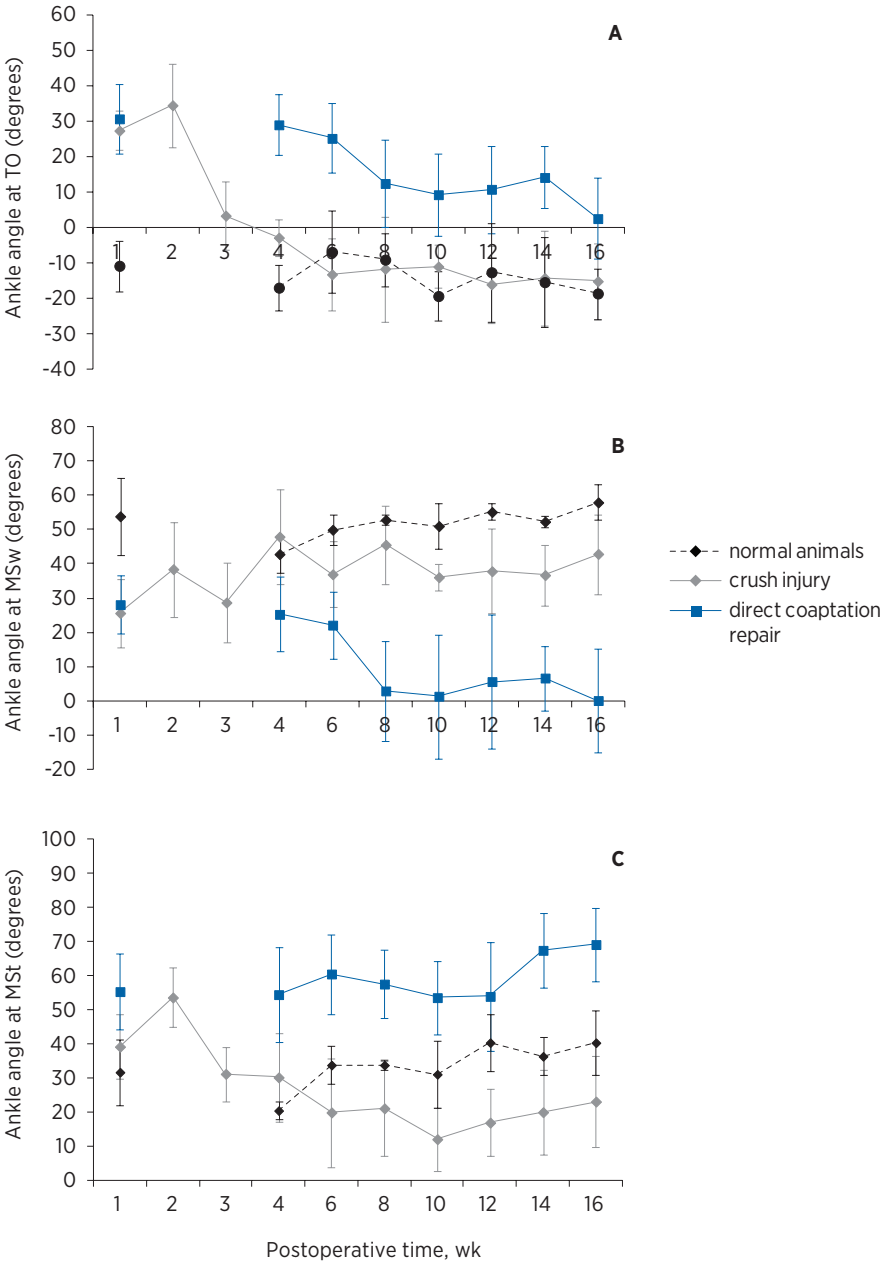

Figure 3

Recovery of ankle angles at toe-off (TO) (A), midswing (MSw) (B), and midstance (MSt) (C) after sciatic nerve crush injury and direct coaptation repair. REsutls for the recovery of ankle angles after autograft repair are not shown because these were not different from the results after direct coaptation repair except the results were more variable after autograft repair (larger SD).

FB profiles represents the total number of tibial motoneurons from which axons had regenerated to the peroneal nerve after injury and repair. Correction for incomplete labeling of peroneal motoneurons by the first DY injection was not necessary because of the high labeling efficacy in normal animals (91% ± 2.4%) The number of single-labeled DY profiles represents the total number of peroneal motoneurons from which axons had regenerated to the tibial nerve branch. No corrections were made for inclusion of nonregenerated peroneal motoneurons because of the high number of profiles from which axons had regenerated to the peroneal nerve: crush injury (401 ± 227), direct suture (342 ± 92) and autograft repair (372 ± 17) (numbers not significantly different from the normal number of peroneal profiles (427 ± 54, ANOVA, P=0.36). The number of double-labeled FB-DY profiles represents the number of correctly directed peroneal motoneurons. Thus, the percentages of correctly directed peroneal motoneurons, calculated for the number of correctly directed profiles (FB-DY) divided by the total number of profiles that was labeled before injury with DY (DY and FB-DY), were 71% ± 4.9% after crush injury, 42% ± 4.2% after direct coaptation repair, and 25% ± 6.6% after autograft repair (P<0.001).

An interesting difference was found in the distribution of differently labeled profiles after crush injury versus transection injury and repair. After crush injury, single-labeled FB and double-labeled FB-DY profiles were more segregated, whereas after direct coaptation and autograft repair, profiles were all intermingled.

2D digital video ankle motion analysis

No contractures of the ankle were present after sciatic crush injury, direct coaptation, or autograft repair. Autotomy was not observed after sciatic crush injury but was seen in 1 animal after direct coaptation and in 2 animals after autograft repair. All ankle angles decreased after sciatic crush injury, direct coaptation, and autograft repair. The angle at TO showed decreased plantar flexion (Figure 3A). The angle at MSw showed decreased dorsiflexion (Figure 3B). The angle at MSt showed decreased ability to support the body weight (Figure 3C).

After sciatic crush injury all angles had recovered to normal values 4 weeks after injury (TO, P=0.45; MSw, P=0.27; MSt, P=0.26). However, after that, the angles at MSt and MSw showed increased plantar flexion compared with normal (P=0.47 and 0.04, respectively, at 14 weeks (Figure 3B and C), but not quite significant at 16 weeks, P=0.09 and P=0.08).

Recovery of the different ankle angles after direct coaptation and autograft repair was incomplete. At the end of the experiment (16 weeks) the angles at TO, MSw, and MSt were still significantly different from normal (direct coaptation repair: TO, P=0.04; MSw, P=0.007; MSt, P=0.25; autograft repair: TO, P=0.01; MSw, P=0.08; MSt, P=0.002). The best recovery was observed for the angle at TO (Figure 3A). Sixteen weeks after direct coaptation repair, the angle had recovered to about 67% of normal (angle TO in normal animals, -15.0°; 1 week after direct coaptation repair, 30°; and 16 weeks after repair, 0°; P=0.003). For the angle at TO, recovery after

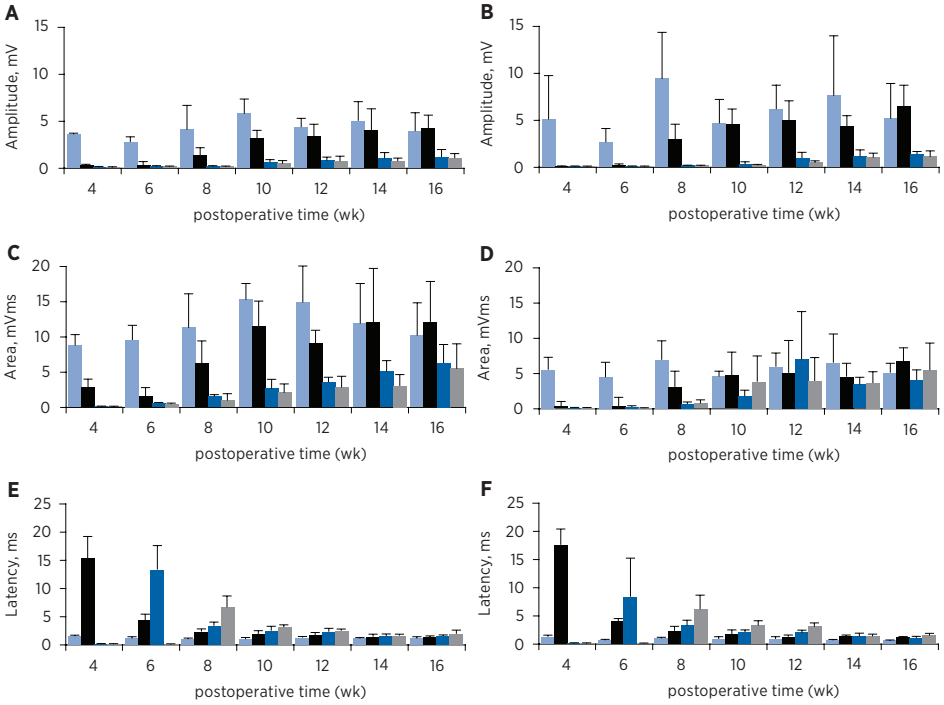

Figure 4

Recovery of compound muscle action potential (CMAP) amplitude (A,B), area (C,D), and latency (E,F) in the plantar (A,C,E) and dorsal foot muscles (B,D,F). Light blue, results for normal animals; black bars, results after crush injury; dark blue bars, results after direct coaptation repair; gray bars, results after autograft repair.

autograft repair was poor (27%; angle at 16 weeks, 17.5°) and not significantly different from that after 1 week (P=0.25).

The angle at MSw decreased further after direct coaptation and autograft repair (Figure 3B); 8 weeks after direct coaptation repair, the angle had decreased even more (-0.83°) compared with the angle 1 week after transection of the nerve (24.7°, P=0.047). Also 8 weeks after autograft repair, the angle had decreased further (17.8°, compared with 28.9° after 1 week), but not significantly (P=0.42). After 8 weeks, the angle at MSt did not change; 16 weeks after direct coaptation repair, the angle (-2.83°) was still significantly different from that at 1 week (P=0.04).

The angle at MSt did not recover significantly over time (Figure 3C): 16 weeks after direct coaptation and autograft repair, the angles (68.6° and 62.3°, respectively) were not significantly different from the angles after 1 week (56.8° and 57.1°, P=0.07 and 0.32)

Compound muscle action potentials

No CMAPs were recorded in the plantar and dorsal foot muscles 1 week after sciatic crush injury, direct coaptation, and autograft repair (Figure 4). The first CMAPs were recorded 4 week after sciatic nerve crush injury and 6 weeks after direct coaptation and autograft repair. The CMAP amplitude in the plantar foot muscles had recovered y 12 weeks after sciatic crush injury (P=0.02 at 10 weeks and P=0.28 at 12 weeks) (Figure 4A). After direct coaptation and autograft repair, CMAP amplitude recovered only slightly, and at the end of the experiment (at 16 weeks) it was still significantly different from that of normal animals (P=0.02 and 0.002, respectively). Similar results were found for CMAP amplitudes recorded in dorsal foot muscles (Figure 4B) and the CMAP areas (Figure 4C and D). The CMAP latency (Figure 4E and F) was increased compared with normal after all types of injury and repair. It decreased again to normal values 12 weeks after sciatic crush injury and 14 weeks after direct coaptation repair (although at the end of the experiment, there still small differences after all types of nerve injury and repair compared with results in normal animals).

Nerve morphometry

After crush injury, the number of myelinated fibers was increased slightly compared with normal (Table 2), but they were also smaller and less myelinated (Figure 5). After direct coaptation and autograft repair, there were more myelinated fibers than after crush injury (direct coaptation repair, P=0.02, but not significantly after autograft repair, P=0.68). These myelinated fibers were also smaller (P<0.001 for crush injury and autograft repair) and less myelinated (although not significantly, P=0.08, and 0.49, respectively).

Table 2

Results for nerve morphometry

	distal to the injury or repair site, mean±SD			
group*	**fascicle area, mm²**	**no. of MF/ fascicle**	**mean MF diameter, mm**	**myelin thickness, mm**
normal†	0.73 ± 0.09	7,650 ± 464	8.02 ± 0.46	1.20 ± 0.09
crush injury	0.486 ± 0.03	9,642 ± 1,184	4.971 ± 0.323	0.737 ± 0.154
direct coaptation repair	0.472 ± 0.051	13,079 ± 1,166	3.729 ± 0.189	0.591 ± 0.056
autograft repair	0.601 ± 0.332	10,058 ± 1,725	3.816 ± 0.199	0.672 ± 0.103

MF, myelinated fiber.

*all groups contained 5 animals.

† results for normal animals are also presented in **Chapter 7**

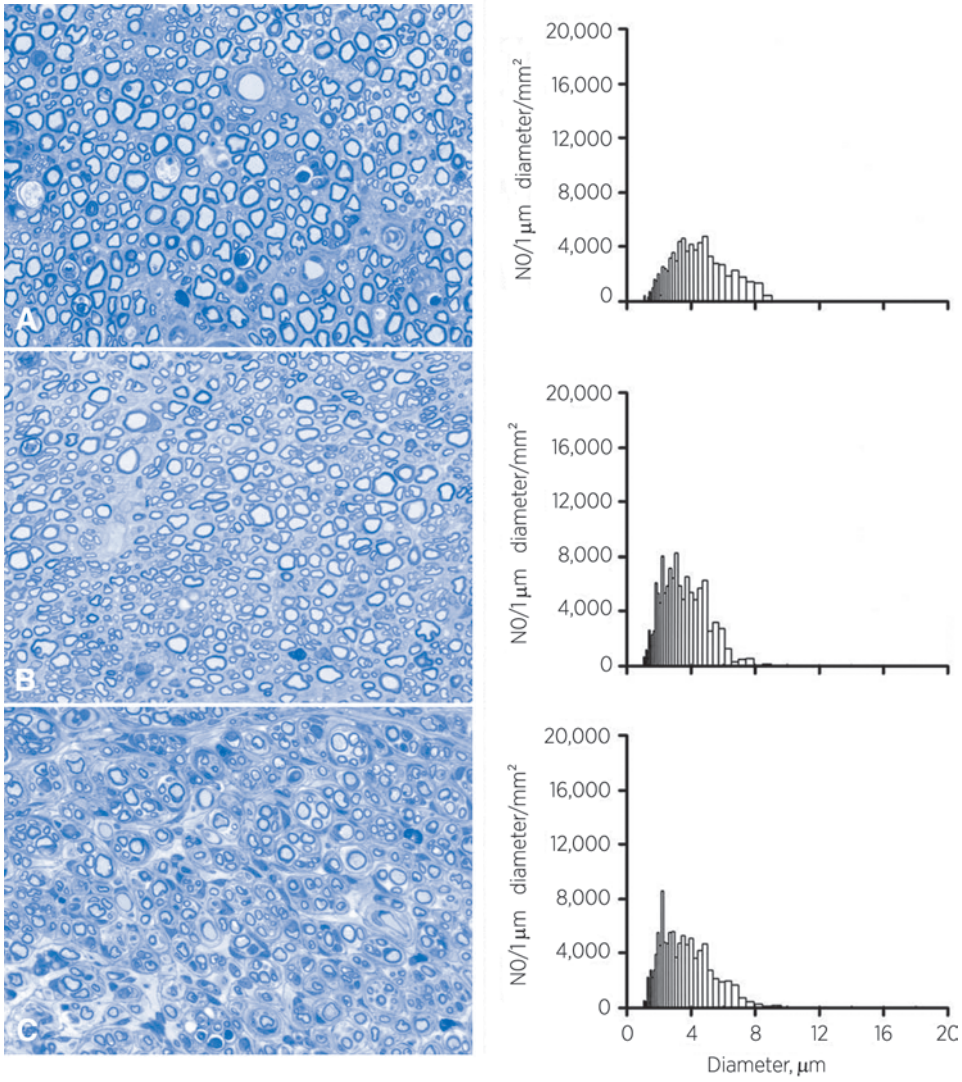

Figure 5
Size distribution of myelinated fibers (MF) after crush injury (A), direct coaptation (B), and autograft repair (C).

Muscle morphometry

After crush injury, the total muscle fiber surface area and mean muscle fiber size were slightly decreased compared with normal (Table 3). After direct coaptation and autograft repair, the total muscle fiber surface area and mean muscle fiber size were even smaller than after crush injury, although not significantly ($P>0.05$ for both comparisons). The number of muscle fibers was similar to the normal number after all types of nerve injury and repair. The distribution of type I and type II fibers, however, had changed after direct coaptation and autograft repair

from predominantly type I in normal soleus muscles to more type II than type I in reinnervated soleus muscles.

Correlations

There were no significant correlations between the percentages of correctly directed peroneal motoneurons and the ankle angles after crush injury, direct coaptation, and autograft repair at 8 weeks (TO, P=0.05; MSw, P=0.49; MSt, P=0.51) or at 16 weeks (TO, P=0.09; MSw, P=0.62; MSt, P=0.33). Also, there were no significant correlations between the quantitative results of regeneration and the ankle angles at 16 weeks (Table 4), except for the mean myelinated diameter and the angle at MSt (r=0.9970 and P=0.0495) and the mean myelin thickness and the angle at MSw (r=0.9999 and P=0.007).

DISCUSSION

To improve functional results for patients with nerve injuries, it is important to investigate different factors that may contribute to recovery. One of these factors includes the number of axons that regenerate. Another important factor is the degree to which the original pathways are restored. In our study, the number of motoneurons whose axons had regenerated to the peroneal nerve after crush injury, direct coaptation, and autograft repair was not significantly different from the normal number of peroneal motoneurons. The number of myelinated fibers was increased after all type of nerve injury and repair. Although other factors (eg, time to reinnervation and quality of the axon) also have to be considered, our study of sequential tracing and ankle motion analysis shows that misdirection of regenerating axons is an important factor that may limit results after nerve injury and repair.

Accuracy of motor axons regeneration

The percentages of correctly directed peroneal motoneurons showed that the accuracy of motor axon regeneration is limited: only 71.4% of the peroneal motoneurons were correctly directed 2 months after the crush injury, 42.0% after direct coaptation repair, and 25.1% after autograft repair. These percentages of correct direction were surprisingly low.

The percentage after crush injury (71%) was low considering that clinical recovery after crush injury is often complete [1]. Also experimentally, scores for the sciatic function index return to normal 4 weeks after a crush injury [31]. This complete recovery of function after crush injury has been explained by guidance of regenerating axons through their original basal lamina tubes [19, 32]. Thus, in our study, misdirection may have been caused damage to the basal lamina tubes by the applied crush technique [33, Varejao, 2004 #143]. Others, however, have also found indications for the presence of some misdirection after crush injury [17, 19, 34].

The percentages after direct coaptation (42.0%) and autograft repair (25%) were low even after maximal attempt to correct fascicular alignment. On the basis of the size of the peroneal motoneuron pool (31% of the rat sciatic nerve [35]) this suggests that regeneration after transection of the nerve occurs at random. Although this finding supports earlier studies that indicated that reinnervation of muscles is nonspecific [7, 8, 11, 36-38] some studies have reported specificity [6, 10, 24]. This discrepancy among different studies may be explained by several factors, including the size of the nerve and technical factors, as discussed below. The mechanism for misdirection, even with correct fascicular alignment, may be explained by dispersion of regenerating axons at the coaptation site, as demonstrated earlier by Ramón y Cajal (1928) (Figure 2A, **Chapter 2**) [39]. Witzel et al. [20] recently confirmed this finding using mice with a fluorescent marker in a subset of their axons and showed that regenerating axons have access to more than 100 basal lamina tubes.

Finally, the lowest percentage of correctly directed peroneal motoneurons after autograft repair can be explained by criss-crossing of regenerating axons at the distal tibial and peroneal coaptation sites, as recently demonstrated by Lutz [40].

Although these percentages provide insight to the accuracy of regeneration after nerve injury and repair and can be used as a baseline for further experiments, additional factors must be considered in the interpretation of the results. First, the size of the nerve must be considered. Puigdellivol-Sanchez et al. [24] recently found a much higher percentage of correctly directed tibial motoneurons (87%), using the same sequential tracing technique, animal model, and time points of evaluation as in our study. The difference (with 42% correctly directed peroneal motoneurons in our study) can be explained at least partly by the relatively larger size of the tibial nerve [35]. Using simultaneous tracing of the tibial (FB) and peroneal (DY) nerves, we found that the sciatic nerve consists of about 61% tibial motoneurons and 39% peroneal motoneurons [26].

Second the time point of evaluation must be considered. Pruning may later correct for misdirection [14, 15]. However, the relative importance of this mechanism in the repair of motor nerves that innervate different muscles has not been determined (see below). Third, the percentages of correctly directed motoneurons may also differ depending on the animal model and age of the animal [41].

Fourth, factors concerning the sequential tracing technique must be considered. We used a technique that was introduced by Puigdellivol-Sanchez et al. [21]. This technique has a high labeling efficiency (91% after 8 weeks in our study) and does not cause marked damage to the nerve; also, there is no significant fading of the first tracer (DY) or blockage of uptake of the second one (FB) [21, 23]. However, a potential problem of the technique might be persistence of DY tracer at the injection site, resulting in an overestimation of the percentage correct direction. Puigdellivol-Sanchez et al. [22] estimated that the last accounts for about 17% of the DY labeling after 8 weeks. Review of their data demonstrated that this was in part due to 1 outlier. After exclusion of this outlier, the percentage decreased to 6%. We grossly determined persistence of DY tracer by examining the distribution of

double-labeled profiles in an area of the anterior horn that is normally occupied exclusively by tibial motoneurons (Figure 2) and found no sign of persistence of tracer.

Another potential problem of this sequential tracing technique is that no distinction can be made between profiles only labeled by the second tracer (FB) as a result of misdirection of tibial axons versus correctly directed peroneal motoneurons not labeled by the first tracer (DY). The technique also cannot distinguish between profiles only labeled by the first tracer (DY) as a result of misdirection of peroneal axons vs peroneal motoneurons that had not regenerated. This was not a problem in our study because of the high labeling efficiency and high total number of regenerated profiles after all types of injury and repair, but is must be considered, for example, in the analysis of repair techniques with lower numbers of regenerated motoneurons. A third tracer applied simultaneously with the second tracer to the tibial nerve branch might solve this problem. Finally, it must be noted that in this study we used an ideal autograft (mixed nerve and size-matched). Results may be different for clinical repair of motor nerves with multiple sensory sural nerve grafts [42].

Recovery of function

Ankle motion analysis showed that misdirection may have an effect on recovery of function. After all 3 types of nerve injury and repair, the balance of ankle plantar and dorsiflexion was disturbed. Two months after crush injury, the angles of plantar flexion at MSt and MSw were increased, confirming previous results of Varejao et al. [43]. After direct coaptation and autograft repair, the maximum angle of dorsiflexion at MSw was decreased further compared with the angle 1 week after transection of the nerve (Figure 3B). This disturbed balance of plantar and dorsiflexion can be explained by the random regeneration of tibial and peroneal motoneurons resulting in a much higher percentage of correctly directed tibial motoneurons than of correctly directed peroneal motoneurons. The tibial motoneuron pool, as mentioned above, is significantly larger than the peroneal motoneuron pool. This random regeneration may even lead to more regenerated tibial than peroneal motoneurons into the peroneal nerve and, thus, to active plantar flexion during the swing phase. However, this was not investigated in our study with simultaneous CMAP recordings.

Ankle motion analysis also showed there probably is little adaptation for misdirected motoneurons; the angle at MSw did not change significantly from 8 to 16 weeks after direct coaptation repair, and at 16 weeks, the angle was still significantly decreased compared with the angle at 1 week after nerve transection. However, a longer period of follow-up may be needed [44]. A mechanism to later correct for misdirection might be initial polyinnervation of muscles by axonal branches from the same motoneuron, followed by pruning of misdirected axon collaterals [44, 45]. This mechanism would also explain the increased number of myelinated fibers after nerve injury and repair that has been found to subsequently decrease

to normal values after 1 year [46]. However, the percentage of motoneurons with multiple projections to different muscles after sciatic nerve injury and repair is low (5.6% 90 days after autograft repair [47]); thus the effect of this mechanism on the recovery of function is questionable.

Another mechanism that may later correct for misdirection is central adaptation. The role of this mechanism after injury and repair remains to be defined. Of note, we found that after sciatic nerve crush injury different labeled profiles were more organized in the anterior horn than they were after direct coaptation and autograft repair. This may have contributed to better functional recovery after crush injury. For example, central adaptation might be better for groups of motoneurons from which axons were misdirected to the same nerve branch than for intermingled motoneurons with correct and incorrect projections. This could also explain the closer to normal distribution of type I and type II muscle fibers after sciatic crush injury compared with more type II than type I fibers after direct coaptation and autograft repair.

Aside from accuracy of regeneration, other factors also contribute to the recovery of function after nerve injury and repair. In our study, CMAPs were recorded earlier after crush injury than after direct coaptation and autograft repair, probably as a result of staggered axonal regeneration across the coaptation site. A shorter period of denervation leads to better muscle [2] and functional recovery. Furthermore, myelinated fibers were smaller and less myelinated after direct coaptation and autograft repair than after crush injury (Figure 5). This combined effect of different factors on the recovery of function can explain that no significant correlations were found in our study between the percentages of correctly directed peroneal motoneurons and the different ankle angles. Nevertheless, this study demonstrates that misdirection of regenerating axons (in addition to the degree of regeneration) is a significant factor that can explain the poor outcome after nerve injury and repair. The results of this study can be used as the baseline for the evaluation of new techniques of nerve repair that may improve the accuracy of regeneration- for example, for nerve tubes with a more advance microarchitecture (multichannel nerve tube)- and the selective application of nerve growth factors.

ACKNOWLEDGEMENTS

We thank LouAnn Gross for her advice on embedding and staining techniques, Tony Koch for his excellent animal care, and Jane Meyer for her secretarial assistance.

REFERENCES

1. Sunderland, S., Nerve injuries and their repair: A critical appraisal. 1991, Melbourne: Churchill Livingstone.
2. Fu, S.Y. and T. Gordon, Contributing factors to poor functional recovery after delayed nerve repair: prolonged denervation. J Neurosci, 1995. 15(5 Pt 2): p. 3886-95.
3. Fu, S.Y. and T. Gordon, Contributing factors to poor functional recovery after delayed nerve repair: prolonged axotomy. J Neurosci, 1995. 15(5 Pt 2): p. 3876-85.
4. Brushart, T., The mechanical and humoral control of specificity in nerve repair. Operative nerve repair and reconstruction. 1991, Philadelphia: J.B. Lippincott. 215-230.
5. Dyck, P.J., et al., Assessment of nerve regeneration and adaptation after median nerve reconnection and digital neurovascular flap transfer. Neurology, 1988. 38(10): p. 1586-91.
6. Politis, M.J., Specificity in mammalian peripheral nerve regeneration at the level of the nerve trunk. Brain Res, 1985. 328(2): p. 271-6.
7. Abernethy, D.A., A. Rud, and P.K. Thomas, Neurotropic influence of the distal stump of transected peripheral nerve on axonal regeneration: absence of topographic specificity in adult nerve. J Anat, 1992. 180 (Pt 3): p. 395-400.
8. Bernstein, J.J. and L. Guth, Nonselectivity in establishment of neuromuscular connections following nerve regeneration in the rat. Exp Neurol, 1961. 4: p. 262-75.
9. Zhao, Q., et al., Specificity of muscle reinnervation following repair of the \ transected sciatic nerve. A comparative study of different repair techniques in the rat. J Hand Surg [Br], 1992. 17(3): p. 257-61.
10. Evans, P.J., et al., Selective reinnervation: a comparison of recovery following microsuture and conduit nerve repair. Brain Res, 1991. 559(2): p. 315-21.
11. Brushart TM, M.M., Alteration in connections between muscle and anterior horn motoneurons after peripheral nerve repair. Science, 1980. 208(9): p. 603-605.
12. Aldskogius, H., et al., Specific and nonspecific regeneration of motor axons after sciatic nerve injury and repair in the rat. J Neurol Sci, 1987. 80(2-3): p. 249-57.
13. Aldskogius, H. and L. Thomander, Selective reinnervation of somatotopically appropriate muscles after facial nerve transection and regeneration in the neonatal rat. Brain Res, 1986. 375(1): p. 126-34.
14. Brushart, T.M., Preferential reinnervation of motor nerves by regenerating motor axons. J Neurosci, 1988. 8(3): p. 1026-31.
15. Brushart, T.M., Motor axons preferentially reinnervate motor pathways. J Neurosci, 1993. 13(6): p. 2730-8.
16. Madison, R.D., S.J. Archibald, and T.M. Brushart, Reinnervation accuracy of the rat femoral nerve by motor and sensory neurons. J Neurosci, 1996. 16(18): p. 5698-703.
17. Bodine-Fowler, S.C., et al., Inaccurate projection of rat soleus motoneurons: a comparison of nerve repair

techniques. Muscle Nerve, 1997. 20(1): p. 29-37.
18. Rende, M., et al., Accuracy of reinnervation by peripheral nerve axons regenerating across a 10-mm gap within an impermeable chamber. Exp Neurol, 1991. 111(3): p. 332-9.
19. Nguyen, Q.T., J.R. Sanes, and J.W. Lichtman, Pre-existing pathways promote precise projection patterns. Nat Neurosci, 2002. 5(9): p. 861-7.
20. Witzel, C., C. Rohde, and T.M. Brushart, Pathway sampling by regenerating peripheral axons. J Comp Neurol, 2005. 485(3): p. 183-90.
21. Puigdellivol-Sanchez, A., et al., Fast blue and diamidino yellow as retrograde tracers in peripheral nerves: efficacy of combined nerve injection and capsule application to transected nerves in the adult rat. J Neurosci Methods, 2000. 95(2): p. 103-10.
22. Puigdellivol-Sanchez, A., et al., Persistence of tracer in the application site--a potential confounding factor in nerve regeneration studies. J Neurosci Methods, 2003. 127(1): p. 105-10.
23. Puigdellivol-Sanchez, A., et al., On the use of fast blue, fluoro-gold and diamidino yellow for retrograde tracing after peripheral nerve injury: uptake, fading, dye interactions, and toxicity. J Neurosci Methods, 2002. 115(2): p. 115-27.
24. Puigdellivol-Sanchez, A., A. Prats-Galino, and C. Molander, Estimations of topographically correct regeneration to nerve branches and skin after peripheral nerve injury and repair. Brain Res, 2006.
25. de Ruiter, G.C., et al., Two-dimensional digital video ankle motion analysis for assessment of function in the rat sciatic nerve model. J Peripher Nerv Syst, 2007. 12(3): p. 216-22.
26. de Ruiter, G.C., et al., Accuracy of motor axon regeneration across autograft, single-lumen, and multichannel poly(lactic-co-glycolic acid) nerve tubes. Neurosurgery, 2008. 63(1): p. 144-53; discussion 153-5.
27. Strasberg, S.R., et al., Wire mesh as a post-operative physiotherapy assistive device following peripheral nerve graft repair in the rat. J Peripher Nerv Syst, 1996. 1(1): p. 73-6.
28. Dyck, P.J., D. P.J.B., and J.K. Engelstad, Pathologic alterations of nerves. Peripheral Neuropathy, ed. D. P. and T. P.K. Vol. 1. 2005, Philadelphia: Elsevier. 733-829.
29. Brooke, M.H. and K.K. Kaiser, Some comments on the histochemical characeterization of muscle adenosine triphosphate. J Histoechem Cytochem, 1969. 17: p. 431-432.
30. Vleggeert-Lankamp, C.L., et al., Type grouping in skeletal muscles after experimental reinnervation: another explanation. Eur J Neurosci, 2005. 21(5): p. 1249-56.
31. Hare, G.M., et al., Walking track analysis: a long-term assessment of peripheral nerve recovery. Plast Reconstr Surg, 1992. 89(2): p. 251-8.
32. de Medinaceli, L., Functional consequences of experimental nerve lesions: effects of reinnervation blend. Exp Neurol, 1988. 100(1): p. 166-78.
33. Beer, G.M., J. Steurer, and V.E. Meyer, Standardizing nerve crushes with a non-serrated clamp. J Reconstr Microsurg, 2001. 17(7): p. 531-4.
34. Swett, J.E., C.Z. Hong, and P.G. Miller, All peroneal motoneurons of the rat survive crush injury but some fail to

reinnervate their original targets. J Comp Neurol, 1991. 304(2): p. 234-52.
35. Swett, J.E., et al., Motoneurons of the rat sciatic nerve. Exp Neurol, 1986. 93(1): p. 227-52.
36. Gillespie, M.J., T. Gordon, and P.R. Murphy, Reinnervation of the lateral gastrocnemius and soleus muscles in the rat by their common nerve. J Physiol, 1986. 372: p. 485-500.
37. Miledi, R. and E. Stefani, Non-selective re-innervation of slow and fast muscle fibres in the rat. Nature, 1969. 222(193): p. 569-71.
38. Weiss, P. and A. Taylor, Further experimental evidence against "neurotropism" in nerve regeneration. J. Exp. Zool., 1944. 95: p. 233-257.
39. Cajal, S., Degeneration and regeneration of the nervous system. London: Oxford University Press, 1928.
40. Lutz, B.S., The role of a barrier between two nerve fascicles in adjacency after transection and repair of a peripheral nerve trunk. Neurol Res, 2004. 26(4): p. 363-70.
41. Robinson, G.A. and R.D. Madison, Developmentally regulated changes in femoral nerve regeneration in the mouse and rat. Exp Neurol, 2006. 197(2): p. 341-6.
42. Sulaiman, O.A., et al., Chronic Schwann cell denervation and the presence of a sensory nerve reduce motor axonal regeneration. Exp Neurol, 2002. 176(2): p. 342-54.
43. Varejao, A.S., et al., Ankle kinematics to evaluate functional recovery in crushed rat sciatic nerve. Muscle Nerve, 2003. 27(6): p. 706-14.
44. Hennig, R. and E. Dietrichs, Transient reinnervation of antagonistic muscles by the same motoneuron. Exp Neurol, 1994. 130(2): p. 331-6.
45. Gorio, A., et al., Muscle reinnervation--II. Sprouting, synapse formation and repression. Neuroscience, 1983. 8(3): p. 403-16.
46. Mackinnon, S.E., A.L. Dellon, and J.P. O'Brien, Changes in nerve fiber numbers distal to a nerve repair in the rat sciatic nerve model. Muscle Nerve, 1991. 14(11): p. 1116-22.
47. Valero-Cabre, A., et al., Superior muscle reinnervation after autologous nerve graft or poly-L-lactide-epsilon-caprolactone (PLC) tube implantation in comparison to silicone tube repair. J Neurosci Res, 2001. 63(2): p. 214-23.